

## Molecular structure and properties of oxime phosphonates: an FTIR and quantum chemical study

R. R. Shagidullin,<sup>a</sup> I. I. Vandyukova,<sup>a\*</sup> E. E. Zvereva,<sup>a</sup> A. O. Vigel',<sup>a</sup> L. I. Shchukina,<sup>a</sup> and R. S. Garaev<sup>b</sup>

<sup>a</sup>A. E. Arbuzov Institute of Organic and Physical Chemistry,  
Kazan Scientific Center, Russian Academy of Sciences,  
8 ul. Akad. Arbuzova, 420088 Kazan, Russian Federation.  
Fax: +7 (843 2) 73 2253. E-mail: helva@iopc.knc.ru

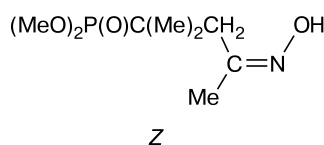
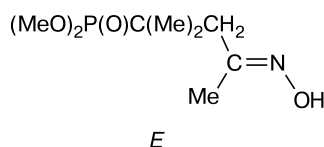
<sup>b</sup>Kazan State Medical University,  
40 ul. Butlerova, 420012 Kazan, Russian Federation.  
Fax: +7 (843 2) 36 0393. E-mail: rector@guk.kcn.ru

Peculiar features of the molecular structure, isomeric composition, and hydrogen bonding in new, potentially physiologically active  $\gamma$ -oxime alkylphosphonates were established.

**Key words:**  $\gamma$ -oxime dimethylphosphonates, difference FTIR spectroscopy, quantum chemical computations, molecular structure.

Compounds containing an oxime fragment can reactivate a vital enzyme cholinesterase inhibited by toxic organophosphorus compounds.<sup>1</sup> A number of 3-oxoalkylphosphonic acid derivatives are non-anticholinesterase compounds of low toxicity and possess the antidote properties (with unusual mechanisms) with respect to poisoning with anticholinesterase agents.<sup>2</sup> To design novel potential antidotes by combining these two types of fragments, investigations on the synthesis and properties of oximes of 3-oxoalkylphosphonates were carried out.

The synthesis of these compounds results in a mixture of *E*- and *Z*-isomers.<sup>3</sup>

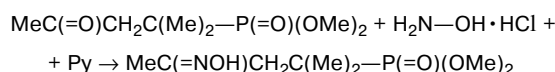


The *E*-isomer was isolated as a single crystal. According to X-ray analysis data, it exists in the form of cyclic H-bonded dimers of the "head-to-tail" type.<sup>3</sup> Since the reactivity of oxime compounds as cholinesterase reactivators depends on their structure,<sup>4</sup> it was of interest to determine the aggregation state, *E/Z* isomer ratio, and specific features of the molecular structure of oxime of 1,1-dimethyl-3-oximinobutylphosphonic acid dimethyl ester (substance

of domestic drug "Dimephosphon") in the solid state and in solutions. However, the investigations were complicated by the fact that only the *E*-isomer was isolated (from product **1**, see below) in individual state from the reaction mixture. Information on the *Z*-isomer was obtained by comparing the IR spectra of product **1** and a polycrystalline mixture enriched with the *Z*-form (product **2**) using quantum chemistry methods.

### Experimental

<sup>31</sup>P NMR spectra of solutions in CH<sub>2</sub>Cl<sub>2</sub> were recorded on a Bruker CXP-100 spectrometer operating at 36.5 MHz. Oxime of 1,1-dimethyl-3-oximinobutylphosphonic acid dimethyl ester was obtained as a mixture of *E*- and *Z*-isomers by the reaction



in 65% yield, m.p. 96–103 °C. Found (%): C, 43.21; N, 6.20; P, 13.95. C<sub>8</sub>H<sub>18</sub>O<sub>4</sub>PN. Calculated (%): C, 43.04; N, 6.27; P, 13.88. <sup>31</sup>P NMR ( $\delta_p$ ): 37.91, 38.50 (integrated intensity ratio is about 85 : 15%). Product **1** was isolated by fractional crystallization from ethyl acetate, m.p. 105–106 °C. <sup>31</sup>P NMR ( $\delta_p$ ): 37.90. After isolation of product **1** and removal of ethyl acetate *in vacuo* the residue (polycrystalline mass enriched with the second isomer) was used as product **2**, m.p. 96–98 °C.

IR spectra of the products under study in the solid state (KBr pellets) and in CH<sub>2</sub>Cl<sub>2</sub> solutions (*C* = 0.1–0.03 mol L<sup>−1</sup>, cell thickness *l* = 0.109–0.407 cm) were recorded on a Bruker Vector-22 FT-IR spectrometer in the 4000–400 cm<sup>−1</sup> range with a resolution of 4 cm<sup>−1</sup>.

All calculations were carried out in the framework of the density functional theory with the B3LYP functional and the

**Table 1.** Scale factors ( $m$ ) used in vibrational frequency calculations of oxime phosphonates

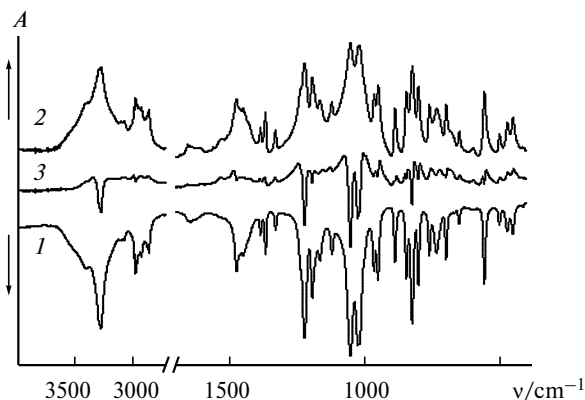
Natural coordinate	Structure element	$m$
Stretching	C—C, C—N, N—O, O—C	0.9207 <sup>7</sup>
	C—P, P—O	1.040 <sup>8</sup>
	P=O	1.022 <sup>8</sup>
	O—H	0.9527 <sup>7</sup>
	C—H	0.889 <sup>8</sup>
Bending	CCC, CCN, CNO, CCP, POC	1.0144 <sup>7</sup>
	CPO, OPO	1.070 <sup>8</sup>
	CCH, OCH	0.950 <sup>7</sup>
	NOH	0.876 <sup>7</sup>
	HCH	0.9016 <sup>7</sup>
Torsion	Any	0.9523 <sup>7</sup>
Out-of-plane deviation	All	0.976 <sup>7</sup>

6-31G\* basis set using the GAUSSIAN-98 program<sup>5</sup> at the Supercomputer Center of Collective Use, Kazan Scientific Center, Russian Academy of Sciences. To correct for systematic errors, the calculated force constants were multiplied by the scale factors  $m$ :  $F_{ij}^m = (m_{ii}m_{jj})^{1/2}F_{ij}$ , where  $F_{ij}$  are the force constants in the dependent natural coordinates<sup>6</sup> and  $m_{ii}$  and  $m_{jj}$  are elements of the scale factor matrix. Since the GAUSSIAN-98 program allows force constant calculations in Cartesian coordinates, subsequent transformation to the natural coordinates and scaling were carried out using a normal coordinate analysis program<sup>7</sup> and then a conventional secular equation  $\mathbf{GF}^m\mathbf{L} = \mathbf{LA}$  was solved<sup>6</sup> using the scale factors listed in Table 1. The scale factors were chosen earlier<sup>8,9</sup> in such a manner that the normal vibrational frequencies calculated in the framework of this approach for a wide variety of molecules correctly reproduce the corresponding experimental data. Evaluation of the scale factor set using data for various compounds including conformationally inhomogeneous ones revealed transferability of these parameters; in addition, the experimentally observed conformational sensitivity of vibrations was reproduced using the same scale factors for different conformers.<sup>9</sup>

## Results and Discussion

The spectrograms of polycrystalline products **1** and **2** (Fig. 1) differ insignificantly. Both of them exhibit well-documented<sup>10,11</sup> key absorption bands  $\nu(\text{OH})$  ( $3300\text{ cm}^{-1}$ ),  $\nu(\text{CH})$  ( $3000\text{--}2850\text{ cm}^{-1}$ ),  $\delta(\text{CH})$  ( $1480\text{--}1300\text{ cm}^{-1}$ ),  $\nu(\text{P=O})$  ( $1230\text{ cm}^{-1}$ ),  $\nu(\text{CC})$  ( $1195\text{ cm}^{-1}$ ),  $\nu(\text{CO})$  ( $1060/1030\text{ cm}^{-1}$ ), and  $\nu(\text{P—O})$  ( $830\text{ cm}^{-1}$ ), as well as some other bands (NO, POC, CNO, CCC) at  $1300\text{ cm}^{-1}$  and at lower frequencies. These parameters are consistent with the structural formulas given above. The  $\nu(\text{C=N})$  absorption bands near  $1650\text{ cm}^{-1}$  are weak and almost indistinguishable against the background (see Fig. 1, spectra *1* and *2*), which is in agreement with the published data.<sup>9,10</sup>

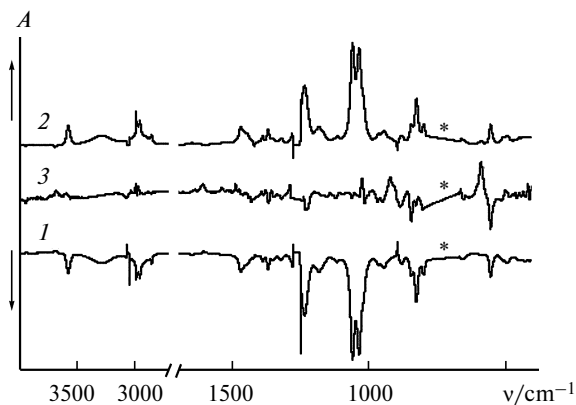
To obtain a more detailed picture and to reveal more subtle effects, we studied the spectra of solutions using

**Fig. 1.** FTIR absorption spectra of products **1** (*1*) and **2** (*2*) as KBr pellets and the difference spectrum (*3*).

difference spectrometry and the results of quantum chemical calculations of the molecular structure and vibrational spectra of the *E*- and *Z*-isomers.

The difference spectrum recorded for the solid phase (see Fig. 1, curve *3*) shows some features indicating different degree of inhomogeneity of the samples and different quantitative characteristics (*E/Z* ratios) of the samples of chemically identical composition (the same vibrational frequencies but different intensities).

The spectrograms of the solutions in  $\text{CH}_2\text{Cl}_2$ , which is a medium of low polarity, are also quite similar (Fig. 2, spectra *1* and *2*). At the same time they allow one to draw some conclusions on the behavior of the oxime hydroxyls. In both cases the absorption bands in the region of  $\nu(\text{OH})$  stretching vibrations are clearly split into a broad component with a maximum at  $\sim 3285\text{ cm}^{-1}$  and a narrow sharp band with a maximum at  $3578\text{ cm}^{-1}$ . The relative intensity of the first component decreases while that of the second component increases with dilution. This is an indication of equilibrium solutions, which also points that the low-frequency component should be attributed to the

**Fig. 2.** FTIR absorption spectra of solutions of products **1** (*1*) and **2** (*2*) in  $\text{CH}_2\text{Cl}_2$  ( $C = 3 \cdot 10^{-2}/\text{mol L}^{-1}$ ,  $l = 0.407\text{ cm}$ ) and the difference spectrum (*3*); the region of strong absorption of the solvent is asterisked.

OH groups involved in the intermolecular hydrogen bond ( $\nu^b(\text{OH})$ ) while the high-frequency component characterizes the "nonbonded/free" OH-groups of the molecules ( $\nu^f(\text{OH})$ ) (quotation marks imply the possibility of interaction with the medium). Previously, the  $\nu(\text{OH})$  bands in the spectra of  $\beta$ -oxime phosphonates<sup>12</sup> in  $\text{CCl}_4$  solutions were observed in nearly the same intervals, namely, at  $\sim 3600$  ( $\nu^f(\text{OH})$ ) and  $\sim 3200\text{--}3280$   $\text{cm}^{-1}$  ( $\nu^b(\text{OH})$ ). Thus, the samples studied in this work show a similar behavior

in solutions. In particular, the  $\nu^f(\text{OH})$  bands of the *Z*- and *E*-isomers almost match each other, which agrees with the results of our vibrational frequency calculations (Table 2) and with the published data.<sup>10</sup> Symmetric shape of the  $\nu^b(\text{OH})$  band at  $\sim 3285$   $\text{cm}^{-1}$  indicates that the *E*- and *Z*-isomers of products **1** and **2** are characterized by the same or very similar frequencies. This is not surprising because here the most probable are H-bonded chains  $\text{OH}\cdots\text{O}=\text{P}$ . The difference spectrum of the solutions in

**Table 2.** Experimental and theoretical IR spectra of *E*- and *Z*-isomers of 1,1-dimethyl-3-oximinobutylphosphonic acid dimethyl ester<sup>a</sup>

Assignment <sup>b</sup> (PED <sup>c</sup> (%))	IR spectra of product <b>1</b> , <sup>c</sup> $\nu/\text{cm}^{-1}$		Calculations (B3LYP/6-31G*), $\nu/\text{cm}^{-1}$ ( <i>A</i> ) <sup>d</sup>		
	KBr	$\text{CH}_2\text{Cl}_2$	<i>E</i> <sub>1</sub>	<i>Z</i> <sub>1</sub>	<i>Z</i> <sub>2</sub>
$\nu(\text{OH})$ (99)	—	3578 m	3669 (71)	3671 (71)	—
$\nu(\text{OH})$ (99)	3406 m.sh	3288 m	—	—	3354 (305)
$\nu(\text{OH})^{\text{InterHB}}$	3290/3274 vs	—	—	—	—
$\nu(\text{CH}_3)$ , $\nu(\text{CH}_2)$ (98—36)	2985—2851 m	—	3007—2862 (3—58), 17 frequencies		
$\nu(\text{C}=\text{N})$ (77)	1645 vw,br	1651 vw,br	1656 (4)	1662 (5)	—
$\nu(\text{C}=\text{N})$ (73)	1610 vw	1607 vw	—	—	1614 (4)
$\delta(\text{CH}_3)$ , $\delta(\text{CH}_2)$ (96—30)	1477—1367 m, w	—	1476—1395 (0—22), 16 frequencies		
$\beta(\text{OH})$ (14)	—	—	—	—	1392 (32)
$\beta(\text{OH})$ (30)	—	—	—	1349 (37)	—
$\omega(\text{CH}_2)$ (40)	—	1356 vw	1342 (16)	1332 (13)	—
$\tau(\text{CH}_2)$ (78)	—	—	—	—	1329(4)
$\beta(\text{OH})$ (40)	1330 w	1323 w	1320 (44)	—	—
$\tau(\text{CH}_2)$ (54)	1292 sh	—	1289 (1)	1275 (18)	—
$\omega(\text{CH}_2)$ (52)	—	—	—	—	1301 (1)
$\nu(\text{P}=\text{O})$ (79)	1236 sh	1235 vs	1272 (127)	1272 (92)	—
$\nu(\text{C}—\text{C})$ (40)	1223 vs	—	1223 (25)	1223 (43)	1249 (21)
$\nu(\text{P}=\text{O})$ (44)	—	—	—	—	1222 (68)
$\nu(\text{C}—\text{C})$ (16)	1195 s	1195 sh	1203 (16)	1204 (17)	1188 (35)
$\rho(\text{CH}_3)$ (89—26)	1182—1167 m	—	1185—1152 (0—40), 5 frequencies		
$\nu(\text{C}—\text{C})$ (24)	1122 m	1119 w	1114 (35)	1112 (27)	1124 (13)
$\nu(\text{C}—\text{O})$ (72)	1053 vs	1060 vs	1057 (292)	1056 (308)	1054 (369)
$\rho(\text{CH}_3)$ (30)	—	—	—	1044 (27)	1044 (66)
$\rho(\text{CH}_3)$ (47)	—	—	—	—	1040 (14)
$\nu(\text{C}—\text{O})$ (63)	1026 vs	1038 vs	1036 (279)	1034 (245)	1027 (224)
$\rho(\text{CH}_3)$ (56)	—	—	1032 (11)	—	—
$\rho(\text{CH}_3)$ (30)	1020 vs	1020 sh	1022 (98)	1025 (96)	—
$\rho(\text{CH}_3)$ (35)	1000 sh	1000 sh	1006 (7)	1008 (9)	1013 (9)
$\nu(\text{N}—\text{O})$ (43)	967 m	968 w	958 (69)	—	959 (42)
$\rho(\text{CH}_3)$ (32), $\nu(\text{C}—\text{C})$ (50)	—	—	—	—	957 (9)
$\nu(\text{C}—\text{C})$ (56)	—	—	—	950 (12)	—
$\rho(\text{CH}_3)$ (53)	953 m	948 w	945 (19)	942 (23)	—
$\nu(\text{C}—\text{C})$ (29)	—	—	940 (18)	—	—
$\nu(\text{N}—\text{O})$ (69)	—	930 sh	—	933 (68)	—
$\nu(\text{C}—\text{C})$ (31)	—	—	—	—	931 (10)
$\nu(\text{C}—\text{C})$ (20), $\nu(\text{N}—\text{O})$ (21)	889 m	882 w	880 (21)	897 (4)	886 (6)
$\nu(\text{C}—\text{C})$ (41)	847 m	845 m	829 (43)	841 (25)	842 (6)
$\nu(\text{P}—\text{O})$ (55)	826 s	827 s	812 (143)	811 (135)	820 (111)
$\nu(\text{C}—\text{C})$ (47), $\nu(\text{P}—\text{O})$ (19)	803 m	801 m	790 (77)	792 (69)	799 (41)
$\nu(\text{C}—\text{C})$ (51), $\nu(\text{P}—\text{O})$ (27)	763 m	770 m	746 (60)	748 (61)	761 (64)
	735 m.br	<i>f</i>	—	—	—
$\beta(\text{C}—\text{C}—\text{C})$ (13)	701 s	<i>f</i>	690 (11)	687 (10)	—

(to be continued)

Table 2 (continued)

Assignment <sup>b</sup> (PED <sup>e</sup> (%))	IR spectra of product 1, <sup>c</sup> v/cm <sup>-1</sup>		Calculations (B3LYP/6-31G*), v/cm <sup>-1</sup> (A) <sup>d</sup>		
	KBr	CH <sub>2</sub> Cl <sub>2</sub>	E <sub>1</sub>	Z <sub>1</sub>	Z <sub>2</sub>
γ(OH) (50)	—	—	—	—	667 (142)
γ(OH) (30), ν(C—P) (20)	—	—	—	—	639 (45)
β(CNO) (18)	651 w	658 w	640 (6)	—	(19)
β(CNO) (41)	—	—	—	—	601 (1)
β(PO <sub>3</sub> ) (28), β(OH) (15)	600 vw	600 vw	—	595 (62)	—
β(CNO) (32)	—	—	—	589 (16)	—
β(CCC) (18)	559 m	554 m	559 (56)	—	579 (1)
β(CCC) (27),	—	—	523 (37)	—	—
γ(C=N) (17), γ(OH) (15)	—	—	—	—	—
β(CCC) (20)	504 w	510 sh	—	504 (22)	496 (26)
β(POC) (42), β(OPO) (30)	473 w	497 m	497 (3)	495 (5)	475 (18)
β(CCC) (25)	455 w	—	449 (16)	443 (7)	—
β(CCC) (35)	—	<i>f</i>	428 (26)	417 (35)	443 (5)
	412 vw	—	—	—	—
γ(OH) (32), β(CCC) (7)	—	<i>f</i>	405 (79)	400 (58)	416 (6)

<sup>a</sup> Since the frequencies in the spectra of products 1 and 2 are the same, listed are only the experimental values for one of them, namely, product 1. Well-documented<sup>10</sup> vibrational frequencies ν, δ and ρ alkyl radicals for each multiplet are given in a single row.

<sup>b</sup> Notations 1: ν is stretching, δ is bending, β is scissoring, γ is out-of-plane deformation, τ is twisting, w is wagging, and ρ is rocking vibrations.

<sup>c</sup> Notations 2: s is strong, vs is very strong, w is weak, vw is very weak, m is medium, sh is shoulder, and br is broad band.

<sup>d</sup> The scaled calculated frequencies and intensities (A/km mol<sup>-1</sup>).

<sup>e</sup> Potential energy distribution.

<sup>f</sup> Regions of strong absorption of the solvent.

CH<sub>2</sub>Cl<sub>2</sub> at equal *C* and *I* (see Fig. 2, curve 3) shows some features similar to those observed in the difference spectrum of the solid samples.

We calculated the molecular structures, energies, and IR spectra of possible conformers of the *E*- and *Z*-isomers (*E*<sub>1</sub> and *Z*<sub>1</sub> isomers without intramolecular hydrogen bond (IntraHB) and *Z*<sub>2</sub> (with IntraHB)) (Fig. 3). The calculated geometric parameters of the energetically most favorable form *E*<sub>1</sub> are in reasonable agreement with the X-ray analysis data (see Ref. 3). Theoretical IR spectra also agree with the experimental spectrograms (see Table 2). Table 2 shows that the frequencies and intensities of some vibrations are different for the three isomers. First of all, as should be expected, the ν(OH) frequencies

for the *Z*<sub>2</sub>-isomer are much lower than for the *E*<sub>1</sub>- and *Z*<sub>1</sub>-isomers. Comparison of the theoretical ν(OH) frequencies of the *Z*<sub>1</sub>- and *E*<sub>1</sub>-isomers with the experimental one (ν<sup>f</sup>(OH) = 3578 cm<sup>-1</sup>) gives a scale factor of 0.975. With allowance for this scale factor the ν<sup>IntraHB</sup>(OH) frequency of *Z*<sub>2</sub> equals 3270 cm<sup>-1</sup> (cf. experimental ν(OH)<sup>InterHB</sup> value of 3285 cm<sup>-1</sup>). However, the intensity of the corresponding band, which is quite symmetric in the spectrum of the CH<sub>2</sub>Cl<sub>2</sub> solution (see Fig. 2), decreases upon dilution of the solution to nearly zero as compared to the internal reference, namely, the ν(CH) peak at 2850 cm<sup>-1</sup>; this is typical of the intermolecular rather than intramolecular hydrogen bond. In the case of thermodynamic equilibrium the estimates for the solu-

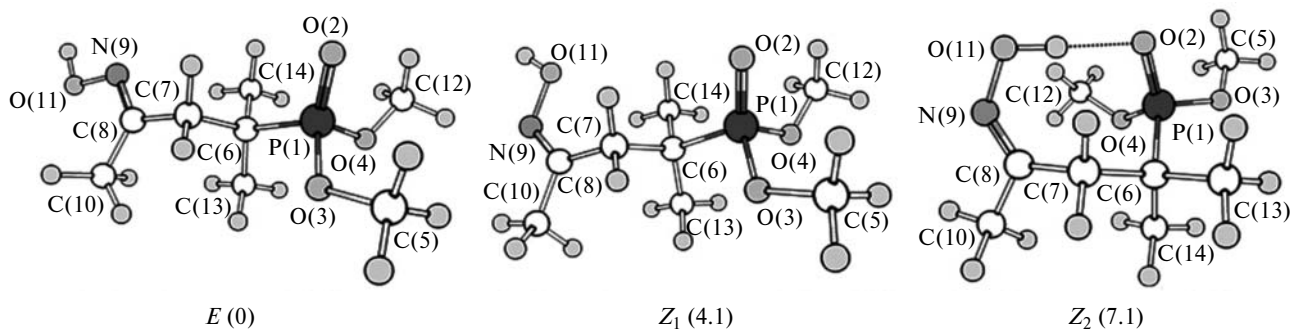


Fig. 3. The most stable molecular forms *E*, *Z*<sub>1</sub>, and *Z*<sub>2</sub> of 1,1-dimethyl-3-oximinobutylphosphonic acid dimethyl ester (according to calculations; relative energies in kJ mol<sup>-1</sup> are given in parentheses).

tions could be obtained using the energies calculated from the following relations<sup>13</sup>

$$N_{Z1}/N_E = \exp[-\Delta E/(RT)] = 0.83,$$

$$N_{Z2}/N_E = \exp[-\Delta E/(RT)] = 0.06.$$

It follows that at room temperature (300 K) the  $E_1 : Z_1 : Z_2^{\text{IntraHB}}$  isomer ratio is 1 (53%) : 0.83 (44%) : 0.06 (3%). However, it should be emphasized that the *E*- and *Z* isomers are geometric isomers rather than conformers that can undergo interconversion under normal conditions. Therefore, the actual *E* : *Z* ratio depends on the synthesis conditions. The theoretical  $Z_1/Z_2$  ratio is practically important and indicates that the  $Z_2$ -isomer can only be present in small amounts.

According to calculations (see Table 2), the vibrational frequencies in the low-frequency region (usually, this is the conformationally more sensitive region) should be attributed to the *E*-isomer (at 523 (optical density  $A = 37$ ), 559 ( $A = 56$ ), 640 ( $A = 6$ ), and 829  $\text{cm}^{-1}$  ( $A = 43$ )) and to the *Z*-isomer (at 589 ( $A = 61$ ), 595 ( $A = 62$ ), and 841  $\text{cm}^{-1}$  ( $A = 25$ )). The fact that these two groups of characteristic bands are detected in the spectra of both products (see Fig. 1 and 2, Table 2) provides a strong proof of non-individual character of the products.

Thus, detailed analysis of experimental spectral data and results of calculations confirmed that products **1** and **2** isolated under experimental conditions represent mixtures of *E*- and *Z*-isomeric oximes with different *E/Z* ratios both in the polycrystalline state and (in agreement with NMR data)<sup>3</sup> in  $\text{CH}_2\text{Cl}_2$  solutions.

The next step was to determine the content and quantitative characteristics of the *E*- and *Z*-isomers as well as (for solutions) H-bonded (with  $\nu^b(\text{OH})$ ) and H-non-bonded (with  $\nu^f(\text{OH})$ ) forms of the molecules. Based on the difference spectra (see Figs 1 and 2, spectra 3) and calculations (see Table 2), we chose two well-separated bands at  $\sim 555$  and  $\sim 600 \text{ cm}^{-1}$  as "fingerprints" of the

*E*- and *Z*-isomers. Other individual bands are distorted by the solvent effects. The common absorption maximum  $\nu(\text{CH})$  at  $2850 \text{ cm}^{-1}$  was treated as internal reference (st). When analyzing molecules with "free" and associated hydroxyl groups in solutions, two clearly different frequencies  $\nu^f(\text{OH})$  and  $\nu^b(\text{OH})$  at 3578 and 3285  $\text{cm}^{-1}$ , respectively, were chosen (see above).

Using the baseline technique, we measured the integrated ( $S$  is the surface area under the spectral contour recorded in the optical density units  $A = \log I_0/I$ ,  $\text{cm}^{-1}$ ) and peak ( $D^{\text{max}}$ ) intensities of the "fingerprint" absorption bands at 600 (*Z*-isomer), 555 (*E*-isomer), 3578 ("free" OH groups) and 3285  $\text{cm}^{-1}$  (associated OH groups) for a series of eight solutions of the products **1** and **2** in  $\text{CH}_2\text{Cl}_2$  (concentrations varied from 0.3 to 0.03  $\text{mol L}^{-1}$ ; cell thickness  $l$  was in the range 0.109–0.407 cm). Correlation analysis<sup>14</sup> showed that these parameters (denoted as  $Y$ ) depend on the concentration  $C$  as  $Y = aC$  (absolute term almost equals to zero) with different correlation coefficients ( $r \approx 1$ ) in the last three cases. Thus, the Buger–Lambert–Beer law is valid. Owing to the low intensity of the *E*-isomer peak at 600  $\text{cm}^{-1}$  the errors in measurements increase; therefore, the parameters were estimated graphically. The integrated ( $\epsilon^S$ ) and peak ( $\kappa^{\text{max}}$ ) extinction coefficients calculated from the relations obtained are equal to 140 and 14, 190 and 10, 740 and 19, and 2080  $\text{L mol}^{-1} \text{ cm}^{-2}$  and 15  $\text{L mol}^{-1} \text{ cm}^{-1}$  for the bands at 555, 600, 3576, 3285  $\text{cm}^{-1}$ , respectively. The errors in determination varied from a few per cent for the  $\nu(\text{OH})$  bands to 10–15% for the  $\nu^Z$  values. Table 3 lists the  $S$  and  $C$  values for the isomers, their monomers and associates in the two pairs of solutions, which illustrate the parameters and their convergence. Processing of the data for other solutions and corresponding correlations gave essentially similar results.

After averaging of the results of measurements it was concluded that products **1** and **2** exist in solution as mixtures of *E*- and *Z*-isomers ( $E : Z = 95 : 5$  for **1** and about

**Table 3.** Data of intensity measurements of the "fingerprint" absorption bands and results of calculations of the content of *E*- and *Z*-isomers of products **1** and **2**, monomeric (f), and H-bonded (b) molecules in  $\text{CH}_2\text{Cl}_2$  solutions using experimental data and correlations obtained in this work\*

Product	$l/\text{cm}$	$S_{555}^E$	$S_{600}^Z$	$C^E$	$C^Z$	$C^{E**}$	$C^{Z**}$	$S_{3578}^f$	$S_{3285}^b$	$C^f$	$C^b$	$C^{f**}$	$C^{b**}$
<b>1</b>	0.280	0.571	0.030	0.029 (97)	0.001 (3)	0.028 (93)	0.002 (7)	4.228	5.966	0.020 (67)	0.010 (33)	0.020 (67)	0.010 (33)
	0.407	2.262	0.053	0.029 (97)	0.001 (3)	0.029 (97)	0.002 (7)	5.501	9.038	0.018 (60)	0.011 (37)	0.020 (67)	0.010 (33)
<b>2</b>	0.280	0.319	0.188	0.025 (83)	0.005 (17)	0.024 (80)	0.006 (20)	4.345	5.968	0.021 (70)	0.010 (33)	0.020 (67)	0.010 (33)
	0.407	1.912	0.278	0.025 (83)	0.005 (17)	0.025 (83)	0.006 (18)	5.675	9.050	0.019 (63)	0.011 (37)	0.020 (67)	0.010 (33)

\* The initial concentration is 0.03  $\text{mol L}^{-1}$ ; the concentrations ( $C$ ) are given in  $\text{mol L}^{-1}$  and in per cent (figures in parentheses).

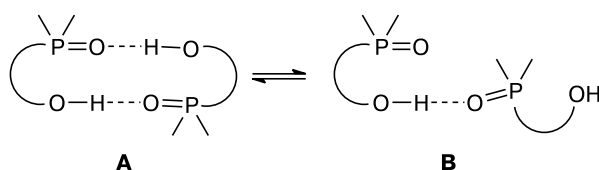
\*\* Concentrations calculated from the peak intensities ( $D^{\text{max}}$ ).

80 : 20 for **2**). Evaluation based on the relative intensities  $A/A^{\text{st}}$  ( $A^{\text{st}}$  is the optical density of the internal reference, the peak at  $2855\text{ cm}^{-1}$ ) lead to nearly the same values. Based on this fact, we determined the  $C^E/C^Z$  ratio and for the starting solid powder products **1** and **2**, which appeared to be equal to the previous estimates. Preferableness of the *E*-isomer revealed in quantum chemical calculations (see above) is thus confirmed experimentally with allowance for the synthesis conditions of the samples in the condensed phase and for the absence of thermodynamic equilibrium between the isomers.

Considering the characteristics of  $\nu^{\text{f}}(\text{OH})$  and  $\nu^{\text{b}}(\text{OH})$  in solutions, correlations analysis showed that the intensity of the band corresponding to the H-bonded hydroxyls tends to zero with dilution (see above). The proportion of the molecules with associated hydroxyl groups is 80% at a concentration of  $0.3\text{ mol L}^{-1}$ , decreases to 60% upon threefold dilution, and then decreases parabolically (see Table 3).

According to X-ray analysis data (see Ref. 3), hydrogen bonds between the *E*-isomer molecules favor the formation of cyclic dimers (**A**). It is natural to assume that this also occurs in solutions. The formation of linear hydrogen bonds between molecules of the same isomer or different isomers (**B**) is also possible. Clearly, steric considerations allow both isomers (*E* and *Z*) to form both cyclic and linear associates. In the latter case, dimeric associates are more preferable because of the constant  $\nu^{\text{b}}$  value for the solutions chosen. Polymeric H-chains should cleave with dilution; this should be accompanied by the appearance of high-frequency bands near the  $\nu^{\text{b}}$  frequencies of the short chains. This suggests the possibility for equilibrium between monomers (see Fig. 3), cyclic dimers (**A**), and linear dimers (**B**) to exist in the solutions of compounds **1** and **2** in  $\text{CH}_2\text{Cl}_2$  (Scheme 1). The observed increase in  $\nu(\text{P}=\text{O})$  from 1223 (in KBr) to  $1235\text{ cm}^{-1}$  is in agreement with involvement of the phosphoryl group in the intermolecular hydrogen bond.

Scheme 1



Relations in the available<sup>15–17</sup> make it possible to calculate the energy of bridging hydrogen bonds  $>\text{C}=\text{N}-\text{OH}\cdots\text{O}=\text{P}$  (or  $\cdots\text{N}$ ). According to Iogansen's "frequency rule",<sup>16</sup> one has  $(\Delta H)^2 = 1.92(\Delta\nu - 40)\text{ kJ mol}^{-1}$ . In our case, one has  $\Delta\nu = 3580 - 3285 = 295\text{ cm}^{-1}$ . Therefore, one H-bridge provides a rather large enthalpy gain ( $\Delta H$ ) of  $22\text{ kJ mol}^{-1}$  ( $5.3\text{ kcal mol}^{-1}$ ), which

is consistent with the corresponding correlations for organophosphorus compounds.<sup>17</sup> A tendency of the oxime phosphonate molecules to undergo H-bond-assisted cyclodimerization is important for prediction of their physiological activity; relevant information is necessary for correct analysis of specific features of biological properties and establishment of corresponding structure—property correlations. Indeed, both most reactive functional centers in cyclic dimers, *i.e.*, the phosphoryl ( $\text{P}=\text{O}$ ) and hydroxyl (oxime hydroxyl  $\text{OH}$ ) groups, become completely or partly self-blocked.

Thus, we have shown that products **1** and **2** exist in the polycrystalline state and in solutions in the solvent of low polarity ( $\text{CH}_2\text{Cl}_2$ ) as mixtures of geometric isomers of molecules with the *anti*- (*E*) and *syn*-orientation (*Z*) of substituents in the oxime fragment and differ in the *E/Z* ratio. The high-melting and readily crystallizable product **1** (single crystals of **1** can be grown) is characterized by the *E* : *Z* isomer ratio of about 95 : 5 (in per cent). Product **2** also contains the *E*-isomer as the major component (*E* : *Z* isomer ratio is about 80% : 20%). Products **1** and **2** both in the solid state and in  $\text{CH}_2\text{Cl}_2$  solutions form intermolecular H-associates of both molecular forms, which decompose to the monomeric form with dilution.

The results obtained are important for further studies under almost *in vivo* conditions, aimed at establishing the action mechanisms and possibility of practical use of the drugs described.

## References

1. S. N. Golikov and S. D. Zaugol'nikov, *Reaktivatory kholinesteraz* [Cholinesterase Reactivators], Meditsina, Leningrad, 1970, 164 pp. (in Russian).
2. B. A. Arbuzov, A. O. Vizel', K. M. Ivanovskaya, I. A. Studentsova, and R. S. Garaev, *Dokl. Akad. Nauk SSSR*, 1968, **182**, 101 [*Dokl. Chem.*, 1968 (Engl. Transl.)].
3. A. O. Vizel', L. I. Shchukina, S. M. Sharipova, I. A. Litvinov, and A. T. Gubaidullin, *Ros. Khim. Zh.*, 1999, **43**, 152 [*Mendeleev Chem. J.*, 1999, **43** (Engl. Transl.)].
4. F. Worek, M. Backer, and H. Thierman, *Hum. Exp. Toxicology*, 1997, **16**, 466.
5. M. J. Frisch, G. W. Trucks, H. B. Schlegel, G. E. Scuseria, M. A. Robb, J. R. Cheeseman, V. G. Zakrzewski, J. A. Montgomery, R. E. Stratmann, J. C. Burant, S. Dapprich, J. M. Millam, A. D. Daniels, K. N. Kudin, M. C. Strain, O. Farkas, J. Tomasi, V. Barone, M. Cossi, R. Cammi, B. Mennucci, C. Pomelli, C. Adamo, S. Clifford, J. Ochterski, G. A. Petersson, P. Y. Ayala, Q. Cui, K. Morokuma, D. K. Malick, A. D. Rabuck, K. Raghavachari, J. B. Foresman, J. Cioslowski, J. V. Ortiz, A. G. Baboul, B. B. Stefanov, G. Liu, A. Liashenko, P. Piskorz, I. Komaromi, R. Gomperts, R. L. Martin, D. J. Fox, T. Keith, M. A. Al-Laham, C. Y. Peng, A. Nanayakkara, C. Gonzalez, M. Challacombe, P. M. W. Gill, B. G. Johnson, W. Chen, M. W. Wong, J. L. Andres, M. Head-Gordon,

- E. S. Replogle, and J. A. Pople, *GAUSSIAN-98, Revision A. 7*, Gaussian, Inc., Pittsburgh (PA), 1998.
6. M. V. Vol'kenshtein, *Stroenie i fizicheskie svoistva molekul*, Izd-vo AN SSSR, Moscow—Leningrad, 1955, 638 pp. (in Russian).
7. J. Baker, A. Jarzecki, and P. Pulay, *J. Phys. Chem. A*, 1998, **102**, 1412.
8. S. A. Katsyuba and E. E. Vandyukova, *Chem. Phys. Lett.*, 2003, **377**, 658.
9. V. A. Sipachev, *J. Mol. Struct.*, 2001, **67**, 567.
10. L. J. Bellamy, *The Infrared Spectra of Complex Molecules*, Methuen and Co., London; John Wiley and Sons Inc, New York, 1957.
11. R. R. Shagidullin, A. V. Chernova, V. S. Vinogradova, and F. S. Mukhametov, *Atlas of IR spectra of Organophosphorus Compounds (Interpreted Spectrograms)*, Nauka Publishers, Moscow; Kluwer Academic Publishers, Dordrecht—Boston—London, 1990, 344 pp.
12. E. P. Trutneva, R. R. Shagidullin, E. E. Borisova, and N. M. Vafina, *Izv. Akad. Nauk SSSR, Ser. Khim.*, 1976, 2616 [*Bull. Acad. Sci. USSR, Div. Chem. Sci.*, 1976, **35** (Engl. Transl.)].
13. *Internal Rotation in Molecules*, Ed. W. J. Orville-Thomas, Wiley, New York, 1974, 329 pp.
14. A. A. Afifi and S. P. Azen, *Statistical Analysis. A Computer Oriented Approach*, Second Edition, Academic Press, New York, 1979, 495 pp.
15. G. C. Pimentel and A. L. McClellan, *The Hydrogen Bond*, Freeman, San Francisco—London, 1960, 475 pp.
16. A. V. Iogansen, *Spectrochim. Acta, Part A*, 1999, **55**, 1582.
17. R. R. Shagidullin, *Adv. Molecular Relaxation Processes*, 1973, **5**, 127.

*Received November 1, 2006;  
in revised form April 10, 2007*